



Multi-objective optimization and analysis of electrical discharge machining process during micro-hole machining of D3 die steel employing salt mixed de-ionized water dielectric

I. Shivakoti^{a,*}, G. Kibria^b, S. Diyaley^a and B. B. Pradhan^a

^aMechanical Engineering Department, Sikkim Manipal Institute of Technology (SMIT), Mazitar, Sikkim-737136, India

^bMechanical Engineering Department, Aliah University Kolkata-700091, India

Article info:

Received: 23/08/2012

Accepted: 10/03/2013

Online: 11/09/2013

Keywords:

Electric discharge machining,

De-ionized water,

D3 die steel,

Dielectric fluid,

Taguchi method.

Abstract

Correct selection of manufacturing condition is one of the most important aspects which should be considered in the majority of manufacturing processes, particularly in the process related to advanced machining process like electrical discharge machining. In electrical discharge machining (EDM), dielectric fluid plays an important role since machining characteristics are greatly influenced by the nature or characteristics of employed dielectric. Moreover, adding various types of abrasives or salt in the fluid at different concentrations also affect the machining performance because of changing dielectric strength property. The present paper addressed the influence of NaNO₃ mixed de-ionized water as a dielectric fluid on micro-hole machining performance criteria such as material removal rate (MRR), tool wear rate (TWR), overcut (OC) and taper during machining of D3 die steel plate.

1. Introduction

Electrical discharge machining (EDM) process has become the workhorse of the tool making industry due to the precise machining of the workpiece that conducts electricity. It plays a major role in machining of dies, tools, etc. made of difficult-to-machine materials like tungsten carbides or hard steels [1]. Although the mechanism of material erosion employed in EDM is still arguable, the widely accepted principle is the conversion of electrical energy into thermal energy through a series of discrete

electrical discharges occurring between the electrode and workpiece immersed in a dielectric fluid [2]. In EDM process, any type of conducting materials can be used as the workpiece material regardless of its hardness. Due to the repetitive spark discharge between the tool and workpiece within a very small gap, the tiny amount of workpiece material is melted and vaporized due to the generation of very high temperature at the spark zone [3]. As machining zone is emmerged in the dielectric fluid, the melted and vaporized materials transform into tiny particles known as debris

*Corresponding author

Email address: ishwar.siwa@gmail.com

upon cooling during the pulse-off time of pulse duration [4, 5]. This debris is removed from the machining zone by the flushing pressure of the dielectric liquid jet. Typically, in EDM, hydrocarbon based oil such as kerosene is used as dielectric fluid. However, in actual practice, these hydrocarbon based fluids show a number of drawbacks during ED machining process. These drawbacks include degradation of hydrocarbon oil at discharge temperature, production of various toxic gases like CH_4 and CO and adhesion of carbon particles onto the tool electrode and workpiece surface that prevents efficient discharge [6, 7]. All these unwanted phenomena obstruct the stable discharge between the tool electrode and workpiece and further results in lower machining efficiency. Therefore, it is very urgent to search out other alternative dielectric fluids, with which these drawbacks can be avoided and machining rate can be enhanced.

For the sake of industrial safety and to ensure green environment during machining in EDM, investigations are going on use other types of dielectric fluids to overcome the above-mentioned disadvantages of hydrocarbon based oil. De-ionized water is one of the supplementary dielectrics that can be used efficiently during machining in EDM [8, 9]. Additionally, investigations performed by many researchers through mixing metal as well as non-metal powder of different sizes of powder particles with different concentration in various dielectrics such as kerosene and de-ionized water have explored their effects on EDM performances and machined surface integrity [10, 11].

Micro-EDM is nothing but a scale-down version of EDM process. In micro-EDM, the range of process parameters is lowered so as to get discharge in a micro-joule range, which can machine hard-to-machine materials in a micro domain (chip or debris size in a micron range) [12, 13]. Numerous investigations have been done to explore effect of de-ionized water on micro-EDM performance and machined surface integrity. Studies have revealed that machining rate can be improved using de-ionized water. However, due to oxygen based oil, it causes thermal wear to the tool electrode. Micro-hole

machining has been also done by several researchers using abrasive mixed de-ionized water [6, 10, 14]. The property of dielectric fluid changes if any additive is mixed in it. The present research studied mixing of NaNO_3 salt at very low concentration and used it as the dielectric fluid during machining of D3 die steel in micro-EDM. Therefore, in the present study, micro electrical discharge machining of D3 die steel was performed to investigate the influence of NaNO_3 salt mixture in de-ionized water on various micro-hole machining performance criteria such as material removal rate, tool wear rate, overcut and taper during micro-EDM process.



Fig. 1. Photographic representation of EDM system using separately developed de-ionized water circulating system.

2. Experimental planning and conditions

The experiments were conducted on a traditional die-sinking EDM machine (ZNC Spark Erosion Machine, Model: ZNC-S-50, Manufactured by Sparkonix India Pvt. Ltd., Pune, India). The machine conventionally uses kerosene as dielectric fluid during machining operation. To facilitate the micro-hole machining using de-ionized water and salt mixed dielectric fluids, a separate dielectric chamber was developed without affecting the existing dielectric supply system of the main machine. The dielectric supply and circulating system were developed using a pump, a

pressure-regulating valve and a pressure gauge. Figure 1 shows schematic view of the developed dielectric supply unit with its various accessories. In this experimentation, the cylindrical shape through micro-holes was machined on D3 die steel plate of dimension 20 mm × 15 mm × 1 mm. Solid cylindrical copper electrodes of diameter 300 μm were used as a tool. Table 1 shows physical as well as mechanical properties of D3 die steel. The experiment was conducted at various concentrations of NaNO₃ salt mixed in de-ionized water. Among the micro-EDM process parameters, peak current and pulse-on-time were the most significant and effective parameters that controlled the EDM process responses in micro-machining domain. Therefore, these two process parameters were varied. Other process parameters, i.e. flushing pressure, duty ratio, polarity, etc. were kept constant. In Table 2, various levels of the three process parameters, namely peak current, pulse-on-time and salt concentration, were listed out. The selection of range of peak current and pulse-on-time was done after literature review of micro-EDM. The proper selection of concentration of salt is very difficult as high concentration of salt results in degradation of dielectric strength of de-ionized water. Therefore, to select the range of different concentration of NaNO₃ salt, many trial experiments were conducted employing NaNO₃ salt mixed de-ionized water dielectric during machining in micro-EDM. Table 3 shows experimental conditions of machining and setting of other process parameters which were kept constant during the experimentation. Taguchi methodology based design of experiments (DOE) was implemented to conduct experiments at various parametric settings. Taguchi methods are statistical methods developed by G. Taguchi to improve the quality of manufacturing goods. Recently, this method can be applied in engineering by technology and various product development applications. According to Taguchi design, nine sets of experiments were performed and each set was repeated three times to reduce the experimental errors. After each run of experimental settings, the micro-EDM response

criteria were measured and calculated for material removal rate (MRR), tool wear rate (TWR) and enlargement of machined micro-hole compared to micro-tool diameter, etc. For higher productivity in machining process, a higher material removal rate (MRR) such as MRR was considered as larger-the-better type problem. The signal-to-noise ratio η (MRR) was calculated as follows:

$$\eta (MRR) = -10 \log_{10}(\text{mean square of reciprocal of MRR}) \quad (1)$$

However, tool wear rate (TWR), overcut (OC), and taper were considered as smaller-the-better type problems since their minimization could improve accuracy of the machined micro-hole. Thus, signal-to-noise ratio η (TWR), η (OC) and η (taper) were calculated as follows:

$$\eta (TWR) = -10 \log_{10}(\text{mean square of reciprocal of TWR}) \quad (2)$$

$$\eta (OC) = -10 \log_{10}(\text{mean square of reciprocal of OC}) \quad (3)$$

$$\eta (\text{taper}) = -10 \log_{10}(\text{mean square of reciprocal of taper}) \quad (4)$$

For better machining performance, larger values of η (MRR), η (TWR), η (OC) and η (taper) are desirable. MRR and TWR were calculated by measuring initial and final weights using a high precision weighing machine (least count: 0.01 mg, make: Mettler Toledo, Switzerland). A measuring microscope manufactured by OLYMPUS, Japan, was used to measure diameters of entry and exit of micro-holes. Micro-hole overcut and taper were calculated as shown in the following equations.

$$\text{Overcut (OC)} = \frac{\text{Entry hole dia.}(D_i) - \text{Tool electrode dia.}(D)}{2} \quad (5)$$

$$\text{Taper} = \frac{\text{entry hole diameter } (D_i) - \text{exit hole diameter } (D_b)}{2 \times \text{material thickness } (L)} \quad (6)$$

Based on the results of various measurements of responses, analysis of these data was

Table 1. Physical and mechanical properties.

Physical Property	Typical Value
Density (g/cm ³)	7.86
Specific heat (Cal/g ⁰ C)	0.110
Thermal conductivity (W/m-K) at 20 ⁰ C	7.2
Tensile strength (Mpa)	640
Elastic modulus (GPa)	190
Hardness Rockwell C	58-64

Table 2. Factors and their levels for experimentation.

Parameters	Unit	Levels		
		L1	L2	L3
Peak current	Amp	0.5	1.0	1.5
Pulse-on-time	μs	8	12	16
Salt concentration	g/lit	1	4	8

Table 3. Experimental conditions for through micro-hole machining on D3 die steel plate.

Conditions	Description
Workpiece (+ve)	20 mm × 15 mm × 1 mm of D3 die steel plate
Electrode (-ve)	Copper micro-tool, 300 μm diameter
Dielectric fluids	De-ionized water
Additive	NaNO ₃ salt
Duty factor (%)	95
Flushing pressure (kgf/cm ²)	0.5
Resistivity of pure de-ionized water (megohm-cm)	4.2

Table 4. Experimental parametric combinations and the corresponding results of responses.

Ex. No.	Input factor			Responses			
	Peak current	Pulse-on time	Salt concentration	Material removal rate (MRR)	Tool wear rate (TWR)	Overcut (OC)	Taper
	Amp	s	g/lit	mg/min	mg/mm	mm	-
1	0.5	8	1	0.0036254	0.0028564	0.067543	0.038950
2	0.5	12	4	0.0048146	0.0018375	0.079255	0.040594
3	0.5	16	8	0.0041571	0.0020001	0.083751	0.051300
4	1	8	4	0.0066324	0.0028744	0.068327	0.056301
5	1	12	8	0.0059013	0.0023112	0.056521	0.061028
6	1	16	1	0.0045245	0.0024347	0.066410	0.064758
7	1.5	8	8	0.0053342	0.0024871	0.072310	0.059551
8	1.5	12	1	0.0065860	0.0033314	0.069640	0.063145
9	1.5	16	4	0.0071350	0.0020466	0.053125	0.065710

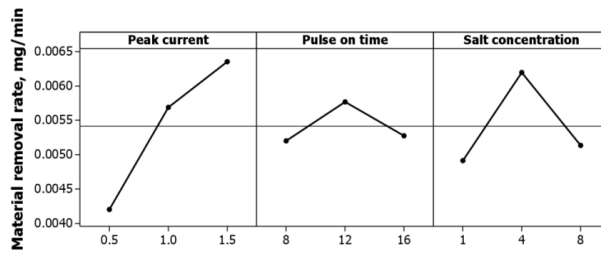


Fig. 2. Main effect plot showing variation of MRR with process parameters.

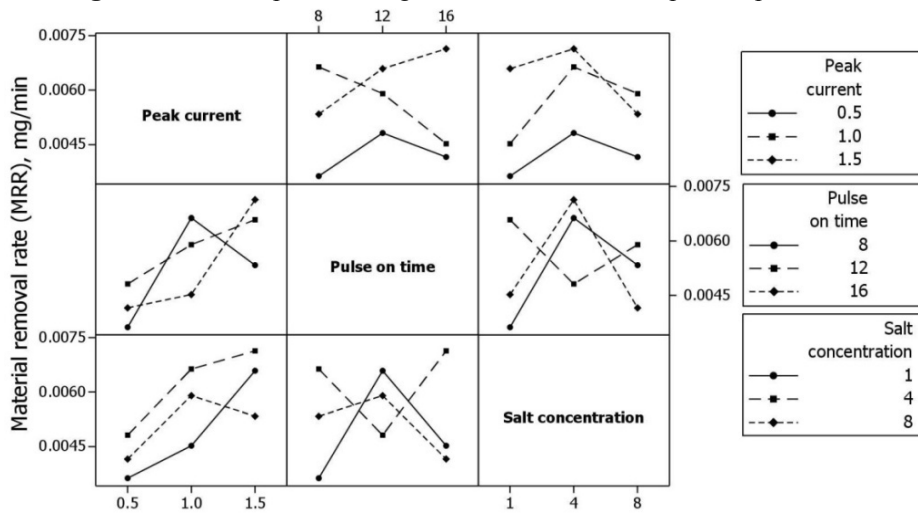


Fig. 3. Parameter interaction plot showing variation of MRR.

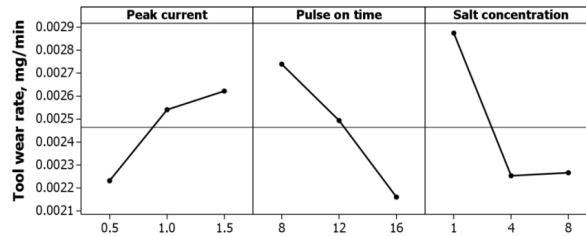


Fig. 4. Main effect plot showing variation of TWR with process parameters.

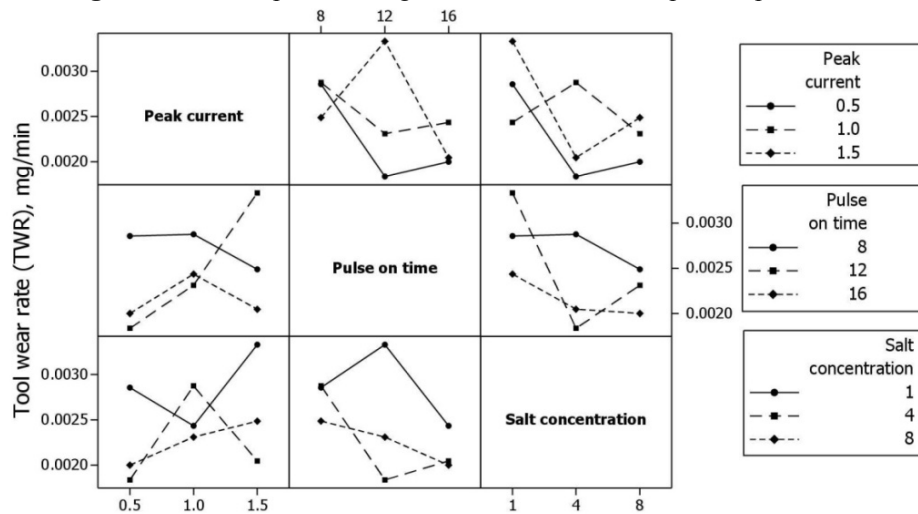


Fig. 5. Parameter interaction plot showing variation of TWR.

done in MINITAB™ software. Table 4 shows parametric combinations of all nine experiments and the corresponding results of responses measured based on the procedures mentioned above. The detailed analysis of the three parameters, namely peak current, pulse-on-time and salt concentration, on the four responses mentioned above are discussed in following section.

3. Results and discussion

3.1. Effects of process parameters on material removal rate (MRR)

Figure 2 shows the main effect plot of material removal rate (MRR) while varying the process parameters at their respective levels. This figure depicts that the machining rates increased sharply as peak current increased from 0.5 to 1.5 Amp. At lower current, a significant portion of the total discharge energy was used to heat the workpiece material and a very less amount of energy was used to vaporise the metal; therefore, the metal removal rate was small. On the other hand, when the discharge current was large such as 1.5 Amp, the discharge energy was quite large and most of the discharge spark was used to melt and vaporize the material, which caused the high degree of material removal from the workpiece. From the same figure, it is also clear that, when pulse-on-time increased from 8 to 12 μ s, MRR increased. However, MRR tended to decrease when pulse-on-time varied from 12 to 16 μ s. As pulse-on-time increased from 8 to 12 μ s, the discharge time duration increased and, as a result, the total energy available for removing the material also increased. Further, at higher pulse-on-time, i.e. at 16 μ s, due to the larger value of pulse duration, metal oxide layer was formed at the discharge zone and this layer prevented uniform and normal discharge between the micro-tool tip and work sample leading to unstable machining condition which in turn decreased MRR. It is also observed in the plot that salt concentration significantly affected MRR. It is evident from the figure that rate of material removal increased sharply as salt concentration increased from 1 to 4 g/lit and decreased when

salt concentration varied from 4 to 8 g/lit. Due to increase of available ions from mixed salt, the uniformity of discharge energy increased between the micro-tool tip and workpiece surface and resulted in increase in material removal rate. However, high salt concentration, i.e. 8 g/lit, resulted in high density of ions available for carrying out discharge in a very small gap between the two electrodes, due to which most of the potential difference was wasted by flowing a current in inter electrode gap without creating significant discharge for material removal. In Fig. 3, the interaction plot of material removal rate with various process parameters such as peak current, pulse-on-time and salt concentration is shown at the considered levels of respective parameters. From this plot, it is evident that there was significant effect of interaction of two varying process parameters while third parameters were kept constant at different levels.

3.2. Effects of process parameters on tool wear rate (TWR)

Figure 4 shows main effect plot for tool wear rate (TWR) at considered levels of various process parameters. It is observed from the plot that peak current had a moderate effect on the TWR. TWR increased when peak current increased from 0.5 to 1.5 Amp. As peak current increased from 0.5 to 1.5 Amp, a small amount of the discharge energy was wasted for local heating of micro-tool material and thermal wear occurred from tool electrode surface. This phenomenon was high enough at high peak current settings. It is observed that TWR sharply decreased in the considered range of pulse-on-time. With increasing value of pulse-on-time, uniform distribution of discharge occurred in the machining gap, which resulted in uniform MRR and there was very small value of energy to be wasted for wear of micro-tool material. Moreover, significant influence of salt concentration on TWR could be observed. According to the plot, TWR decreased when the salt concentration increased from 1 to 4 g/lit and it remained almost constant for further increase in salt concentration; i.e. within the range of 4 to 8 g/lit value. Due to

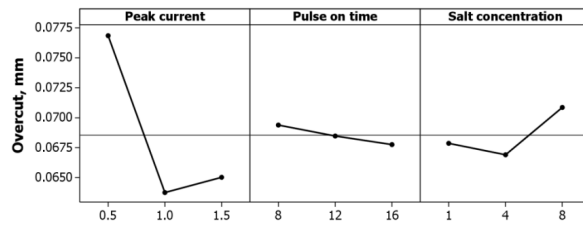


Fig. 6. Main effect plot showing variation of OC with process parameters.

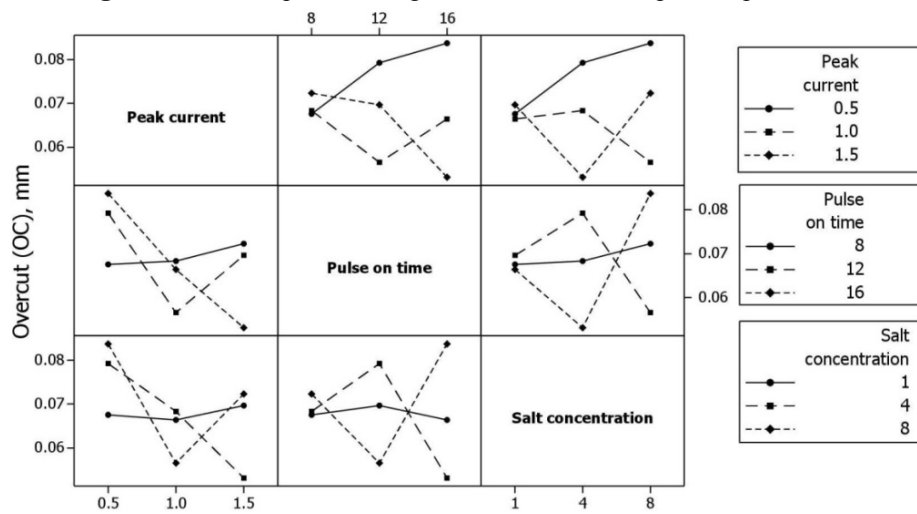


Fig. 7. Parameter interaction plot showing variation of OC.

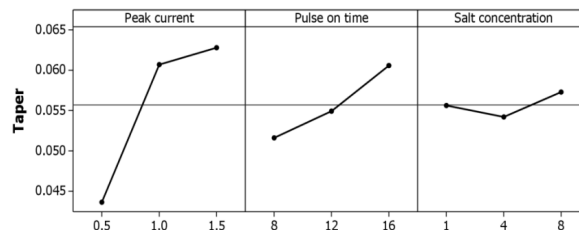


Fig. 8. Main effect plot showing variation of taper with process parameters.

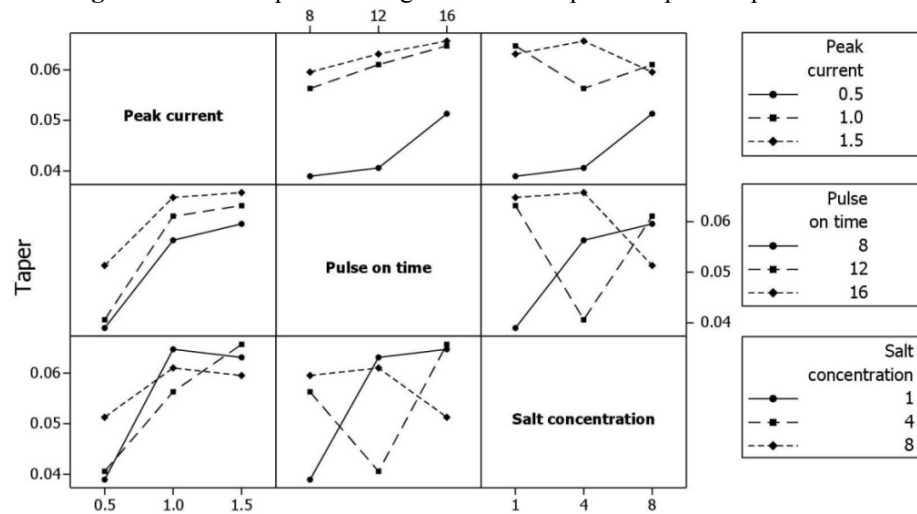


Fig. 9. Parameter interaction plot showing variation of taper.

huge amount of ions available in the very small gap of discharge, the uniform distribution of discharge occurred, due to which there was a very less amount of energy wasted for thermal wear of the micro-tool. Figure 5 shows parametric interaction plot of tool wear rate accounted at various levels of considered process parameters. It is observed that the simultaneous variation of any two process parameters resulted in significant variation of tool wear while the third parameters were kept constant at different considered levels.

3.3. Effects of process parameters on overcut (OC)

Variation of overcut of micro-hole produced by various process parameters during machining is shown in Fig. 6. The main effect plot of OC depicts that overcut of micro-hole decreased sharply with peak current. Minimum overcut was obtained corresponding to the discharge current of 1 Amp. As the peak current increased, energy density of the discharge also increased. In this condition, the debris particle was disintegrated into tinier debris particles. The small sized debris particles easily came out of the narrow passage between the micro-tool and wall of the micro-hole; thus, decreasing chances of secondary sparking and mechanical scratching of the inside wall of micro-hole and resulting in lower OC. However, at higher peak current setting, i.e. at 1.5 Amp, the overcut was high, which was due to the fact that, at high discharge energy, size of debris was high and, while ejecting out from the micro-hole, secondary sparking phenomenon occurred and material from the entry side hole wall. From the same plot, it could be observed that pulse-on-time had no influence on OC. It could be also seen from the graph that effect of salt concentration on OC was not highly significant. However, the overcut was slightly increasing with the increasing levels of salt concentration due to high machining rate at higher concentrations. The parameter interaction plot of overcut for variation of any two process parameters while keeping the third constant at its different levels is shown in Fig. 7. It is obvious from this plot that the simultaneous

variation of any two process parameters had a very significant effect on OC.

3.4. Effects of process parameters on taper

Effects of variation of different process parameters on taper are depicted in Fig. 8. It is observed in this main effect plot that taper of the micro-hole increased with increase in the considered peak current range of 0.5 to 1 Amp. Minimum taper of micro-hole was found at peak current of 0.5 Amp. At low peak current setting, the low value of discharge energy caused uniform material removal with a very small size of debris/crater and reduced degree of taper. However, the taper increased as the peak current increased, which was because, at high peak current settings, the secondary sparking occurred frequently. From the same plot, it is observed that the taper increased with the increase in pulse-on-time from 8 to 16 μ s. With the increase in pulse-on-time, the pulse duration increased which directly increased the amount of discharge energy per unit time discharge and more materials were removed from the workpiece surface. It can be also observed from this main effect plot that the salt concentration had an insignificant effect on taper. The interaction plot of simultaneous variation of the considered process parameters is shown in Fig. 9. Accordingly, there was no such significant effect of interaction for peak current with pulse-on-time and salt concentration. However, other interactions were significant in terms of variation in taper.

4. Analysis of variance (ANOVA) and optimal conditions

Analysis of Variance was performed in order to estimate analysis accuracy of the considered process responses, i.e. MRR, TWR, OC and taper, and to determine relative significance of different process parameters on responses. Tables 5 to 8 show Analysis of variance (ANOVA) test results for the above-mentioned responses, respectively. By comparing these test results and the calculated F-values with standard F-values of ANOVA, it could be concluded that peak current had significant

Table 5. Analysis of Variance (ANOVA) test for material removal rate (MRR).

Source	DF	Seq SS	Adj SS	Adj MS	F
Peak current	2	0.000073	0.000073	0.000036	5.58
Pulse-on-time	2	0.000006	0.000006	0.000003	0.44
Salt concentration	2	0.000028	0.000028	0.000014	2.16
Error	2	0.000013	0.000013	0.000007	
Total	8	0.000120			

Table 6. Analysis of Variance (ANOVA) test for tool wear rate (TWR).

Source	DF	Seq SS	Adj SS	Adj MS	F
Peak current	2	0.000003	0.000003	0.000001	0.70
Pulse-on-time	2	0.000005	0.000005	0.000003	1.39
Salt concentration	2	0.000008	0.000008	0.000004	2.07
Error	2	0.000003	0.000004	0.000002	
Total	8	0.000019			

Table 7. Analysis of Variance (ANOVA) test for overcut (OC).

Source	DF	Seq SS	Adj SS	Adj MS	F
Peak current	2	0.0003130	0.0003130	0.0001565	0.77
Pulse-on-time	2	0.0000040	0.0000040	0.0000020	0.01
Salt concentration	2	0.0000256	0.0000256	0.0000128	0.06
Error	2	0.0004067	0.0004067	0.0002034	
Total	8	0.0007493			

Table 8. Analysis of Variance (ANOVA) test for taper.

Source	DF	Seq SS	Adj SS	Adj MS	F
Peak current	2	0.0006644	0.0006644	0.0003322	99.09
Pulse-on-time	2	0.0001239	0.0001239	0.0000620	18.49
Salt concentration	2	0.0000144	0.0000144	0.0000072	2.14
Error	2	0.0000067	0.0000067	0.0000034	
Total	8	0.0008094			

Table 9. Optimum parametric combinations for the responses.

Responses	Peak current	Pulse-on-time	Salt concentration
Material removal rate (MRR)	1.5 Amp	12 μ s	4 g/lit
Tool wear rate (TWR)	0.5 Amp	16 μ s	4 g/lit
Overcut (OC)	1 Amp	16 μ s	4 g/lit
Taper	0.5 Amp	8 μ s	4 g/lit

contribution to MRR and taper. However, pulse-on-time had the highest contribution to taper. Salt concentration had the highest contribution to tool wear rate. The optimal parametric combinations which provided maximum material removal rate, minimum tool wear rate, minimum overcut and minimum taper are shown in Table 9.

5. Regression analysis

The most important and necessary step for process parameter optimization in any manufacturing process is to understand the principles governing the process by developing an explicit mathematical model. Here, statistical regression technique was utilized to model the micro-EDM process. The following regression equations were developed based on the experimental results, shown in Table 4.

$$\begin{aligned} \text{MRR} = & 0.00752 - 0.00459 \times x_1 - 0.000755 \times x_2 \\ & + 0.00236 \times x_3 + 0.000864 \times x_1x_2 - \\ & 0.000082 \times x_2x_3 - 0.00111 \times x_1x_3 \end{aligned} \tag{7}$$

$$\begin{aligned} \text{TWR} = & 0.00253 + 0.00252 \times x_1 - 0.000045 \times x_2 \\ & - 0.000272 \times x_3 - 0.000127 \times x_1x_2 + \\ & 0.000019 \times x_2x_3 - 0.000075 \times x_1x_3 \end{aligned} \tag{8}$$

$$\begin{aligned} \text{OC} = & 0.0132 + 0.0818 \times x_1 + 0.00635 \times x_2 - \\ & 0.0080 \times x_3 - 0.00788 \times x_1x_2 + 0.000385 \times \\ & x_2x_3 + 0.00152 \times x_1x_3 \end{aligned} \tag{9}$$

$$\begin{aligned} \text{Taper} = & 0.0156 + 0.0138 \times x_1 + 0.00107 \times x_2 + \\ & 0.0070 \times x_3 + 0.00093 \times x_1x_2 - 0.000331 \\ & \times x_2x_3 - 0.00244 \times x_1x_3 \end{aligned} \tag{10}$$

Here, x_1 , x_2 and x_3 correspond to the process parameters peak current, pulse-on-time and salt concentration, respectively, and $0.5 \leq x_1 \leq 1.5$ (Amp), $8 \leq x_2 \leq 16$ (μ s) and $1 \leq x_3 \leq 8$ (g/lit).

6. Multi-objective optimization using grey relational analysis (GRA)

Grey relational analysis (GRA) is one of the powerful and effective soft-tools to analyze various processes which have multiple performance characteristics. In most of the real

world problems, the situation comes in a state which is neither perfectly black (with no information) nor perfectly white (with complete information). This condition is then described as grey. The GRA is based on a grey system, in which a part of information is known and another remaining part is unknown [15]. Generally, GRA is carried out for solving complicated problems which have interrelationships among the designated performance characteristics. GRA is also performed to solve multi-input and discrete data problems effectively and efficiently. In the following sections, the step-by-step procedure of carrying out grey relational analysis is discussed, which shows the grey relational analysis based results of the present research.

6.1. Normalization of experimental results

Normalization is the process in which transformation of input data takes place into an evenly distributed data in a scale range between 0 and 1. The experimental results for the responses MRR, TWR, OC and taper of micro-hole were normalized using Eqs. (11- 12), where x_{ij} is normalized value of y_{ij} for response j ($j = 1,2,3,\dots, n$) of experiment i ($i = 1,2,3,\dots, m$).

If the response is of higher-the-better type, then, the normalized value x_{ij} is expressed as

$$x_{ij} = \frac{(y_{ij} - \min(y_{ij}))}{(\max(y_{ij}) - \min(y_{ij}))} \tag{11}$$

If the response is of smaller-the-better type, then the normalized value x_{ij} is expressed as

$$x_{ij} = \frac{(\max(y_{ij}) - y_{ij})}{(\max(y_{ij}) - \min(y_{ij}))} \tag{12}$$

If the normalized value x_{ij} for a response j of experiment i is equal to 1 or closer to 1, then, it is said that the performance of that particular experiment i is best for the response j . That normalized value is termed as reference value.

(x_{0j}) for j th response. The normalized values of the process responses at each parametric combination of machining are shown in Table 10.

Table 10. Normalization values of the results.

Expt no.	Normalized value			
	MRR	TWR	OC	Taper
1	0.00000	0.31815	0.52924	1.00000
2	0.33903	1.00000	0.14680	0.99686
3	0.15156	0.89149	0.00000	0.97643
4	0.85669	0.30609	0.50364	0.00000
5	0.64843	0.68318	0.88914	0.95787
6	0.25641	0.60013	0.56623	0.95075
7	0.48689	0.56530	0.37358	0.96068
8	0.84358	0.00000	0.46076	0.95383
9	1.00000	0.86001	1.00000	0.94894

Table 11. Grey relational co-efficient and grey grade values.

Expt no.	Grey relational coefficient				Grey relational grade	Order
	MRR	TWR	OC	Taper		
1	0.33333	0.42306	0.51506	1.00000	0.56786	8
2	0.43067	1.00000	0.36949	0.99376	0.69848	3
3	0.37079	0.82167	0.33333	0.95498	0.62019	5
4	0.77723	0.41879	0.50182	0.33333	0.50779	9
5	0.58715	0.61213	0.81852	0.92228	0.73502	2
6	0.40206	0.55564	0.53546	0.91033	0.60087	6
7	0.49352	0.53491	0.44388	0.92709	0.59986	7
8	0.76170	0.33333	0.48112	0.91546	0.62291	4
9	1.00000	0.78126	1.00000	0.90733	0.92215	1

Table 12. Influence of process parameters at different levels on grey relational grade.

Parameters	Average grey relational grade by factor level			Max-min
	Level 1	Level 2	Level 3	
Peak current	0.62884	0.61456	0.71497	0.10040
Pulse on time	0.55850	0.68546	0.71440	0.15590
Salt concentration	0.59721	0.70947	0.65169	0.11226
Mean value of the grey relational grade = 0.6527945				

Table 13. Comparison between initial level and optimal level.

	Raw data	Optimal parametric combinations	
		Prediction	Experiment
Setting level	A ₁ B ₁ C ₁	A ₃ B ₃ C ₂	A ₂ B ₂ C ₃
MRR	0.00362	0.00713	0.00590
TWR	0.00285	0.00205	0.00231
OC	0.06754	0.05313	0.05652
Taper	0.03895	0.06571	0.06103
Grey relational grade	0.56786	0.92215	0.73502
Improvement of grey relational grade = 0.08765			
Percentage of improvement = 25.45 %			

6.2. Grey relational coefficient (GRC)

The grey relational coefficient is calculated to determine closeness of x_{ij} to x_{0j} . Higher value of grey relational coefficient means x_{ij} is closer to x_{0j} . Grey relational coefficient is calculated based on Eq. (13).

$$\gamma(x_{0j}, x_{ij}) = (\Delta_{\min} + \xi\Delta_{\max}) / (\Delta_{ij} + \xi\Delta_{\max}) \quad (13)$$

for $i = 1, 2, 3, \dots, m$ and $j = 1, 2, 3, \dots, n$

where, $\Delta_{ij} = |x_{0j} - x_{ij}|$

$$\Delta_{\min} = \min \{ \Delta_{ij}, i = 1, 2, 3, \dots, m; j = 1, 2, 3, \dots, n \}$$

$$\Delta_{\max} = \max \{ \Delta_{ij}, i = 1, 2, 3, \dots, m; j = 1, 2, 3, \dots, n \}$$

ξ = distinguishing coefficient, $\xi \in (0, 1)$

The normalized values summarized in Table 10 were used to calculate the grey relational coefficient using Eq. (13) and the results are summarized in Table 11. The distinguishing coefficient ξ was taken as 0.5.

6.3. Grey relational grade

Grey relational grade is the weighted sum of the grey relational coefficients for a particular experiment and is calculated using Eq. (14).

$$\Gamma(X_0, X_i) = \sum_{j=1}^n w_j \cdot \gamma(x_{0j}, x_{ij}) \quad (14)$$

for $i = 1, 2, 3, \dots, m$. Here, $\Gamma(X_0, X_i)$ is grey relational grade between comparability sequence X_i and reference sequence X_0 and $\sum_{j=1}^n w_j = 1$.

If the experiment has the highest grey relational grade, then it is said that the experiment would be best choice. In Table 11, the grey relational grade calculated using Eq. (14) is shown for each experimental run. The influence of process parameters at different level and comparison of initial level with optimal level are shown in Tables 12 and 13, respectively. According to this table, it is obvious that the multi-objective optimization parametric combination for producing high accurate micro-hole (least OC and taper) with maximum productivity (highest

MRR and least TWR) had 1.5 Amp peak current, 16 μ s pulse-on-time and 4 g/lit salt concentration.

7. Conclusions

In the present research, attempts were made to machine micro-hole on D3 die steel using EDM set-up based on Taguchi methodology employing NaNO_3 mixed de-ionized water as dielectric at different concentrations. It was seen from the experimental results that great influence of salt concentration in de-ionized water as dielectric in micro-EDM process was observed. The following cases are the major conclusions that can be drawn based on the experimental results achieved in the present research.

1. The influence of various machining process parameters such as peak current, pulse-on-time and salt concentration on performance criteria like MRR, TWR, OC and micro-hole taper was examined while micro-hole machining of steel D3 by EDM technique. Peak current had significant effect on material removal rate and taper while pulse-on-time had significant effect on tool wear rate and taper. Salt concentration had contributing effect on MRR and OC.

2. For multi-objective optimization of response criteria, grey relational analysis (GRA) was performed and the optimal multi-objective process parametric combination using NaNO_3 salt mixed de-ionized water as dielectric had 1.5 Amp peak current, 16 μ s pulse-on-time and 4 g/lit salt concentration.

From the optimal multi-objective process parametric combination achieved by grey relational analysis, it was found that, during multi objective optimization, the percentage improvement for obtaining the best machining setting and optimum parametric combination was 25.45% for de-ionized water during machining of D3 steel in micro-EDM.

The results achieved in the present research could be effectively utilized to produce quality and accurate shaped micro-hole by micro-EDM process utilizing salt mixed de-ionized water dielectric. Moreover, the present findings would open new directions for producing micro-holes

on hard-to-machine steels like D3 in micro-components in micro-engineering applications.

References

- [1] T. Sato, T. Mizutani and K. Kawata, "Electro-discharge machine for micro-hole drilling", *Natl. Techn. Rep.*, Vol. 31, pp. 725-733, (1985).
- [2] C. Van Ossenbruggen, "Micro-spark erosion", *Philips Technisch Tijdschrif*, Vol. 20, pp. 200-213, (1969).
- [3] A. Pandey and S. Singh, "Current research trends in variants of Electrical Discharge Machining: A review", *Int. J. Engg. Sc. Technol.*, Vol. 2, No. 6, pp. 2172-2191, (2010).
- [4] D. T. Pham, S. S. Dimov, S. Bigot, A. Ivanov and K. Popov, "Micro-EDM-recent developments and research issues", *J. Mater. Process. Technol.*, Vol. 149, pp. 50-57, (2004).
- [5] K. H. Ho and S. T. Newman, "State of the art electrical discharge machining (EDM)", *Int. J. Mach. Tool Manuf.*, Vol. 43, pp. 1287-1300, (2003).
- [6] G. Kibria, B. R. Sarkar, B. B. Pradhan and B. Bhattacharyya, "Comparative study of different dielectrics for micro-EDM performance during micro-hole machining of Ti-6Al-4V alloy", *Int. J. Adv. Manuf. Technol.*, Vol. 48, pp. 557-570, (2003).
- [7] Q. H. Zhang, R. Du, J. H. Zhang and Q. Zhang, "An investigation of ultrasonic-assisted electrical discharge machining in gas", *Int. J. Mach. Tool Manuf.*, Vol. 46, pp. 1582-1588, (2006).
- [8] S. L. Chen, B. H. Yan and F. Y. Huang, "Influence of kerosene and distilled water as dielectrics on the electric discharge machining characteristics of Ti-6Al-4V", *J. Mater. Process. Technol.*, Vol. 87, pp. 107-111, (1999).
- [9] H. M. Chow, L. D. Yang, C. T. Lin and Y. F. Chen, "The use of SiC powder in water as dielectric for micro-slit EDM machining", *J. Mater. Process. Technol.*, Vol. 195, pp. 160-170, (2008).
- [10] H. K. Kansal, S. Singh and P. Kumar, "Technology and research developments in powder mixed electric discharge machining (PMEDM)", *J. Mater. Process. Technol.*, Vol. 184, pp. 32-41, (2007).
- [11] M. Y. Ali, N. A. B. Abdul Rahman and E.B. Mohamad Aris, "Powder mixed micro electro discharge milling of titanium alloy: Investigation of material removal rate", *Adv. Mater. Res.*, Vol. 383-390, pp. 1759-1763, (2011).
- [12] O. Y. Kagaya and K. Yada, "Micro-electro discharge machining using water as a working fluid-1: microhole drilling", *Prec. Eng.*, Vol. 8, pp. 157-162, (1986).
- [13] Z. Y. Yu, K. P. Rajurkar and H. Shen, "High Aspect Ratio and Complex Shaped Blind Micro Holes by Micro EDM", *Ann. CIRP*, Vol. 51, pp. 359-362, (2012).
- [14] S. Singh and A. Bhardwaj, "Review to EDM by Using Water and Powder-Mixed Dielectric Fluid", *J. Min. Mater. Charac. Engg.*, Vol. 10, pp. 199-230, (2011).
- [15] J. Deng, "Introduction to grey system theory", *J. Grey Sys.*, Vol. 1, pp. 1-24, (1989).